International Journal of Environment & Agricultural Science

Khalid Elyas Mohamed Elameen Alkhidir, Int J Environ & Agri Sci 2019, 3:2
3: 023

Research

Work Fractal Dimension for Characterizing Shajara Reservoirs of the Permo-Carboniferous Shajara Formation, Saudi Arabia

Khalid Elyas Mohamed Elameen Alkhidir[1*]

[1]*Department of Petroleum and Natural Gas Engineering, College of Engineering, King Saud University, Saudi Arabia*

Abstract

The quality and assessment of a reservoir can be documented in details by the application of Work. This research aims to calculate fractal dimension from the relationship among Work, maximum Work and wetting phase saturation and to approve it by the fractal dimension derived from the relationship among capillary pressure and wetting phase saturation. Two equations for calculating the fractal dimensions have been employed. The first one describes the functional relationship between wetting phase saturation, Work, maximum Work and fractal dimension. The second equation implies to the wetting phase saturation as a function of capillary pressure and the fractal dimension. Two procedures for obtaining the fractal dimension have been utilized. The first procedure was done by plotting the logarithm of the ratio between Work and maximum Work versus logarithm wetting phase saturation. The slope of the first procedure = 3- Df (fractal dimension). The second procedure for obtaining the fractal dimension was determined by plotting the logarithm of capillary pressure versus the logarithm of wetting phase saturation. The slope of the second procedure = Df -3. On the basis of the obtained results of the fabricated stratigraphic column and the attained values of the fractal dimension, the sandstones of the Shajara reservoirs of the Shajara Formation were divided here into three units.

Keywords: Shajara Reservoirs; Shajara Formation; Work Fractal Dimension; Capillary Pressure Fractal Dimension

Introduction

Seismo electric effects related to electro kinetic potential, dielectric permitivity, pressure gradient, fluid viscosity, and electric conductivity was first reported by [1]. Capillary pressure follows the scaling law at low wetting phase saturation was reported by [2]. Seismo electric phenomenon by considering electro kinetic coupling coefficient as a function of effective charge density, permeability, fluid viscosity and electric conductivity was reported by [3]. The magnitude of seismo electric current depends porosity, pore size, zeta potential of the pore surfaces, and elastic properties of the matrix was investigated by [4]. The tangent of the ratio of converted electic field to pressure is approximately in inverse proportion to permeability was studied by [5]. Permeability inversion from seismo electric log at low frequency was studied by [6]. They reported that, the tangent of the ratio among electric excitation intensity and pressure field is a function of porosity, fluid viscosity, frequency, tortuosity, fluid density and Dracy permeability. A decrease of seismo electric frequencies with increasing water content was reported by [7]. An increase of seismo electric transfer function with increasing water saturation was studied by [8]. An increase of dynamic seismo electric transfer function with decreasing fluid conductivity was described by [9]. The amplitude of seismo electric signal increases with increasing permeability which means that the seismo electric effects are directly related to the permeability and can be used to study the permeability of the reservoir was illustrated by [10]. Seismo electric coupling is frequency dependent and decreases expontialy when frequency increases was demonstrated by [11]. An increase of permeability with increasing pressure head and bubble pressure fractal dimension was reported by [12,13]. An increase of geometric and arithmetic relaxation time of induced polarization fractal dimension with permeability increasing and grain size was described by [14,15,16]. An increase of seismo electric field fractal dimension with increasing permeability and grain

***Corresponding Author:** Khalid Elyas Mohamed Elameen Alkhidir, Department of Petroleum and Natural Gas Engineering, College of Engineering, King Saud University Saudi Arabia, E-Mail: kalkhidir@ksu.edu.sa

Sub Date: March 26th 2019, **Acc Date:** April 4th 2019, **Pub Date:** April 4th 2019

Citation: Khalid Elyas Mohamed Elameen Alkhidir (2019) Work Fractal Dimension for Characterizing Shajara Reservoirs of the Permo-Carboniferous Shajara Formation, Saudi Arabia. Int J Environ & Agri Sci 3:023.

size was described by [17]. An increase of resistivity fractal dimension with increasing permeability and grain size was illustrated by [18]. An increase of electro kinetic fractal dimension with increasing permeability and grain size was demonstrated by [19]. An increase of electric potential energy with increasing permeability and grain size was defined by [20] . An increase of electric potential gradient fractal dimension with increasing permeability and grain size was defined by [21]. An increase of differential capacity fractal dimension with increasing permeability and grain size was described by [22].

Material and Method

Sandstone samples were collected from the surface type section of the Permo-Carboniferous Shajara Formation, latitude 26° 52' 17.4", longitude 43° 36' 18". (Figure 1). Porosity was measured on collected samples using mercury intrusion Porosimetry and permeability was derived from capillary pressure data. The purpose of this paper is to obtain Work fractal dimension and to confirm it by capillary pressure fractal dimension. The fractal dimension of the first procedure is determined from the positive slope of the plot of logarithm of the ratio of Work to maximum Work log (work1/4/Work1/4max) versus log wetting phase saturation (logSw). Whereas the fractal dimension of the second procedure is determined from the negative slope of the plot of logarithm of log capillary pressure (log Pc) versus logarithm of wetting phase saturation (log Sw).

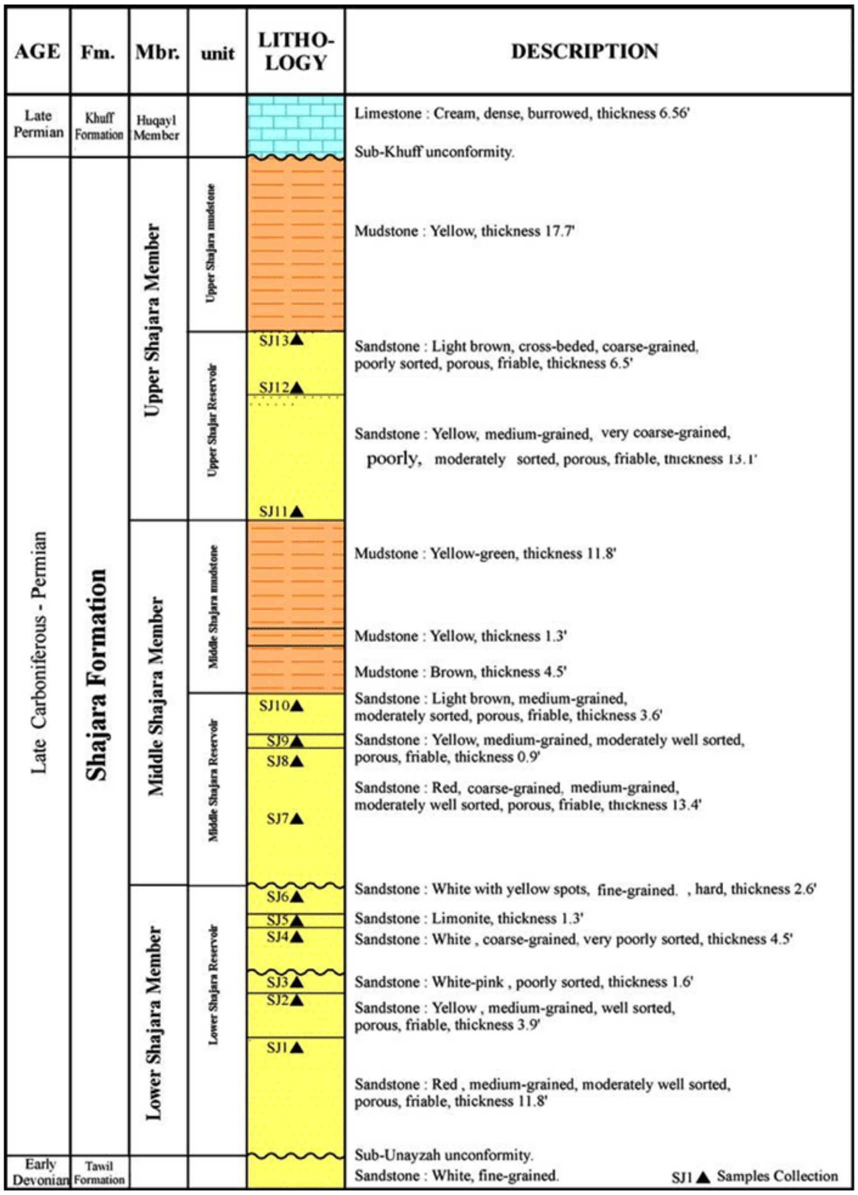

Figure 1. surface type section of the Shajara Reservoirs of the Permo-Carboniferous Shajara Formation, latitude 26° 52' 17.4", longitude 43° 36' 18".

The work can be scaled as

$$Sw = \left[\frac{\mathbf{Work}^{\frac{1}{4}}}{\mathbf{Work}_{\max}^{\frac{1}{4}}} \right]^{[3-\mathbf{Df}]} \qquad [1]$$

Where Sw the water saturation, Work the Work in Joule, Workmax the maximum work in Joule and Df the fractal dimension.

Equation 1 can proofed from

$$V = C_{EK} * E \qquad [2]$$

Where V the velocity in meter / second, CEK the electro kinetic coefficient in ampere/pascal*meter, and E the electric field in volt / meter.

The electric field can be scaled as

$$\mathbf{E} = \left[\frac{\mathbf{v}}{\mathbf{L}} \right] \qquad [3]$$

Where E the electric field in volt /meter, v the electric potential in volt, and L the length in meter.

Insert equation 3 into equation 2

$$\mathbf{V} = \mathbf{C}_{\mathbf{EK}} * \left[\frac{\mathbf{v}}{\mathbf{L}} \right] \qquad [4]$$

The electric potential can be scaled as

$$\mathrm{V} = \left[\frac{Work}{q} \right] \qquad [5]$$

Where v the electric potential in volt, Work in Joule, and q the electric charge in coulomb.

Insert equation 5 into equation 4

$$V = C_{EK} * \left[\frac{Work}{L * q} \right] \qquad [6]$$

The velocity V can be scaled as

$$V = \left[\frac{Q}{A} \right] \qquad [7]$$

Where V the velocity in meter / second, Q the flow rate in cubic meter / second, and A the area in square meter.

Insert equation 7 into equation 6

$$\left[\frac{Q}{A} \right] = C_{EK} * \left[\frac{Work}{L * q} \right] \qquad [8]$$

The flow rate Q can be scaled as

$$Q = \left[\frac{3.14 * \mathrm{r4} * \Delta \mathrm{P}}{8 * \mu * 1} \right] \quad [9]$$

Where Q the flow rate in cubic meter / second, r the pore radiud in meter, ΔP the differential pressure in pascal, μ the fluid viscosity in pascal * second, and l the capillary length in meter.

Insert equation 9 into equation 8

$$\left[\frac{3.14 * \mathrm{r}^4 * \Delta \mathrm{P}}{8 * \mu * 1 * \mathrm{A}} \right] = \mathrm{C}_{\mathrm{EK}} * \left[\frac{\mathrm{Work}}{\mathrm{L*q}} \right] \quad [10]$$

The maximum pore radius can be scaled as

$$\left[\frac{3.14 * \mathrm{r}_{\max}^4 * \Delta \mathrm{P}}{8 * \mu * 1 * \mathrm{A}} \right] = \mathrm{C}_{EK} * \left[\frac{\mathrm{Work}_{\max}}{\mathrm{L*q}} \right] [11]$$

Divide equation 10 by equation 11

$$\left[\frac{\dfrac{3.14 * \mathrm{r}^4 * \Delta \mathrm{P}}{8 * \mu * 1 * \mathrm{A}}}{\dfrac{3.14 * \mathrm{r}_{\max}^4 * \Delta \mathrm{P}}{8 * \mu * 1 * \mathrm{A}}} \right] = \left[\frac{\mathrm{C}_{\mathrm{EK}} * [\dfrac{\mathrm{Work}}{L * \mathrm{q}}]}{\mathrm{C}_{\mathrm{EK}} * [\dfrac{\mathrm{Work}_{\max}}{L * \mathrm{q}}]} \right] \quad [12]$$

Equation 12 after simplification will become

$$\left[\frac{\mathbf{r}^4}{\mathbf{r}_{\max}^4} \right] = \left[\frac{\mathbf{Work}}{\mathbf{Work}_{\max}} \right] \quad [13]$$

Take the fourth root of equation 13

$$\sqrt[4]{\left[\frac{\mathbf{r}^4}{\mathbf{r}_{\max}^4} \right]} = \sqrt[4]{\left[\frac{\mathbf{Work}}{\mathbf{Work}_{\max}} \right]} \quad [14]$$

Equation 14 after simplification will become

$$\left[\frac{\mathbf{r}}{\mathbf{r}_{\max}} \right] = \left[\frac{\mathbf{Work}^{\frac{1}{4}}}{\mathbf{Work}_{\max}^{\frac{1}{4}}} \right] \quad [15]$$

Take the logarithm of equation 15

$$\log \left[\frac{\mathbf{r}}{\mathbf{r}_{\max}} \right] = \log \left[\frac{\mathbf{Work}^{\frac{1}{4}}}{\mathbf{Work}_{\max}^{\frac{1}{4}}} \right] \quad [16]$$

$$\mathbf{But};\log\log\left[\frac{\mathbf{r}}{\mathbf{r}_{\max}}\right]=\left[\frac{\log\log\mathbf{Sw}}{3-\mathbf{Df}}\right] \qquad [17]$$

Insert equation 17 into equation 16

$$\left[\frac{\log\mathbf{Sw}}{3-\mathbf{Df}}\right]=\log\left[\frac{\mathbf{Work}^{\frac{1}{4}}}{\mathbf{Work}_{\max}^{\frac{1}{4}}}\right] \qquad [18]$$

Equation 18 after log removal will become

$$\mathbf{Sw}=\left[\frac{\mathbf{Work}^{\frac{1}{4}}}{\mathbf{Work}_{\max}^{\frac{1}{4}}}\right]^{[3-\mathbf{Df}]} \qquad [19]$$

Equation 19 the proof of equation 1 which relate water saturation, Work, maximum Work, and the fractal dimension

The capillary pressure can be scaled as

$$\mathbf{Sw}=\left[\mathbf{Df}-3\right]*\mathbf{Pc}*\mathbf{constant} \quad [20]$$

Where Sw the water saturation, Pc the capillary pressure and Df the fractal dimension.

Results and Discussion

Based on field observation the Shajara Reservoirs of the Permo-Carboniferous Shajara Formation were divided here into three units as described in Figure1.These units from bottom to top are: Lower Shajara Reservoir, Middle Shajara reservoir, and Upper Shajara Reservoir. Their attained results of the Work fractal dimension and capillary pressure fractal dimension are exhibited in Table 1. Based on the achieved results it was found that the Work fractal dimension is equal to the capillary pressure fractal dimension. The maximum value of the fractal dimension was found to be 2.7872 allocated to sample SJ13 from the Upper Shajara Reservoir as verified in Table 1. Whereas the minimum value of the fractal dimension 2.4379 was reported from sample SJ3 from the Lower Shajara reservoir as shown in Table1. The Work fractal dimension and capillary pressure fractal dimension were detected to increase with increasing permeability as proofed in Table1 owing to the possibility of having interconnected channels.

Table 1 Petrophysical model showing the three Shajara Reservoir Units with their corresponding values of Workfractal dimension and capillary pressure fractal dimension

Formation	Reservoir	Sample	Porosity %	k (md)	Positive slope of the first procedure Slope=3-Df	Negative slope of the second procedure Slope=Df-3	Workfractal dimension	Capillary pressure fractal dimension
Permo-Carboniferous Shajara Formation	Upper Shajara Reservoir	SJ13	25	973	0.2128	-0.2128	2.7872	2.7872
		SJ12	28	1440	0.2141	-0.2141	2.7859	2.7859
		SJ11	36	1197	0.2414	-0.2414	2.7586	2.7586
	Middle Shajara Reservoir	SJ9	31	1394	0.2214	-0.2214	2.7786	2.7786
		SJ8	32	1344	0.2248	-0.2248	2.7752	2.7752
		SJ7	35	1472	0.2317	-0.2317	2.7683	2.7683
	Lower Shajara Reservoir	SJ4	30	176	0.3157	-0.3157	2.6843	2.6843
		SJ3	34	56	0.5621	-0.5621	2.4379	2.4379
		SJ2	35	1955	0.2252	-0.2252	2.7748	2.7748
		SJ1	29	1680	0.2141	-0.2141	2.7859	2.7859

The Lower Shajara reservoir was symbolized by six sandstone samples (Figure 1), four of which label as SJ1, SJ2, SJ3 and SJ4 were carefully chosen for capillary pressure measurement as proven in Table1. Their positive slopes of the first procedure log of the Work to maximum Work versus log wetting phase saturation (Sw) and negative slopes of the second procedure log capillary pressure (Pc) versus log wetting phase saturation (Sw) are clarified in Figure 2, Figure 3, Figure 4, Figure 5 and Table 1. Their Work fractal dimension and capillary pressure fractal dimension values are revealed in Table 1. As we proceed from sample SJ2 to SJ3 a pronounced reduction in permeability due to compaction was described from 1955 md to 56 md which reflects decrease in Work fractal dimension from 2.7748 to 2.4379 as quantified in table 1. Again, an increase in grain size and permeability was proved from sample SJ4 whose Work fractal dimension and capillary pressure fractal dimension was found to be 2.6843 as described in Table 1.

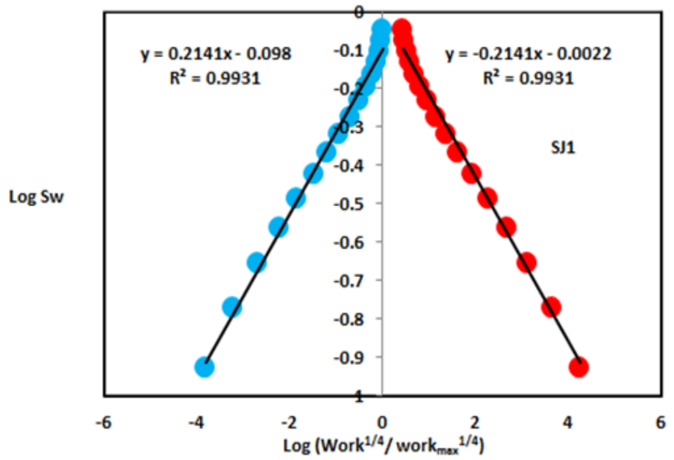

Figure 2. Log (Work$^{1/4}$/Work$^{1/4}_{max}$) & log Pc versus log Sw of sample SJ1

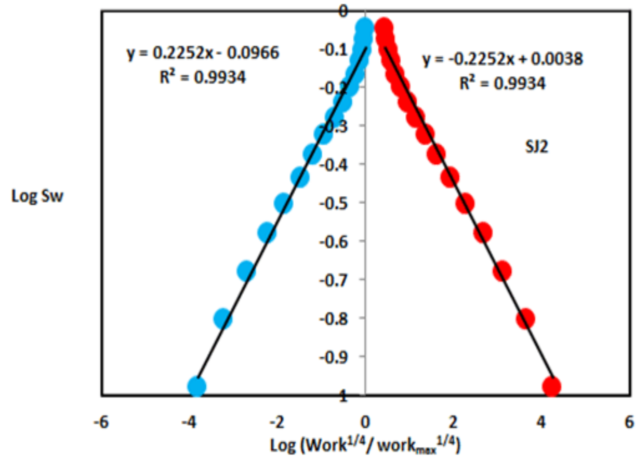

Figure 3. Log (Work$^{1/4}$/Work$^{1/4}_{max}$) & log Pc versus log Sw of sample SJ2

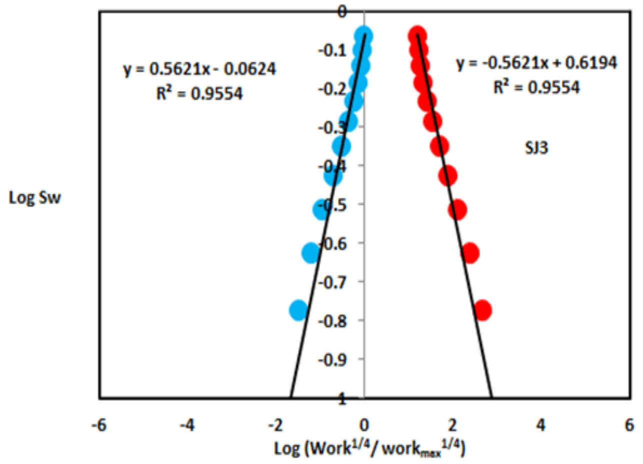

Figure 4. Log (Work$^{1/4}$/Work$^{1/4}_{max}$) & log Pc versus log Sw of sample SJ3

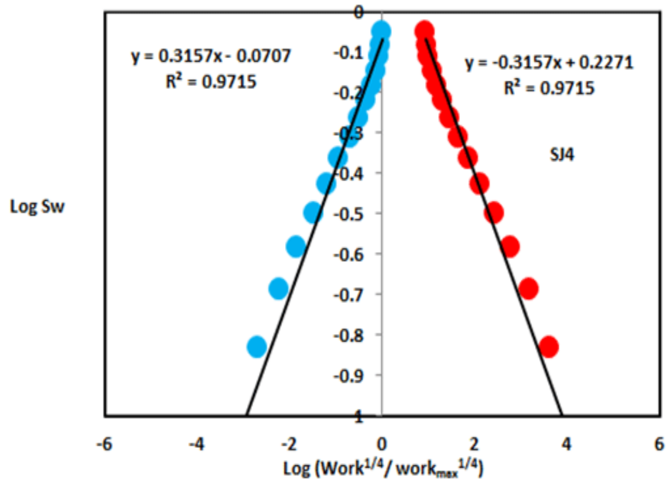

Figure 5. Log (Work$^{1/4}$/Work$^{1/4}_{max}$) & log Pc versus log Sw of sample SJ4

In contrast, the Middle Shajara reservoir which is separated from the Lower Shajara reservoir by an unconformity surface as revealed in Figure 1. It was nominated by four samples (Figure 1), three of which named as SJ7, SJ8, and SJ9 as illuminated in Table1 were chosen for capillary measurements as described in Table 1. Their positive slopes of the first procedure and negative slopes of the second procedure are shown in Figure 6, Figure 7 and Figure 8 and Table 1. Furthermore, their Work fractal dimensions and capillary pressure fractal dimensions show similarities as defined in Table 1.Their fractal dimensions are higher than those of samples SJ3 and SJ4 from the Lower Shajara Reservoir due to an increase in their permeability as explained in table 1.

On the other hand, the Upper Shajara reservoir was separated from the Middle Shajara reservoir by yellow green mudstone as shown in Figure 1. It is defined by three samples so called SJ11, SJ12, SJ13 as explained in Table 1. Their positive slopes of the first procedure and negative slopes of the second procedure are displayed in Figure 9, Figure 10 and Figure 11 and Table 1. Moreover, their Work fractal dimension and capillary pressure fractal dimension are also higher than those of sample SJ3 and SJ4 from the Lower Shajara Reservoir due to an increase in their permeability as simplified in table 1.

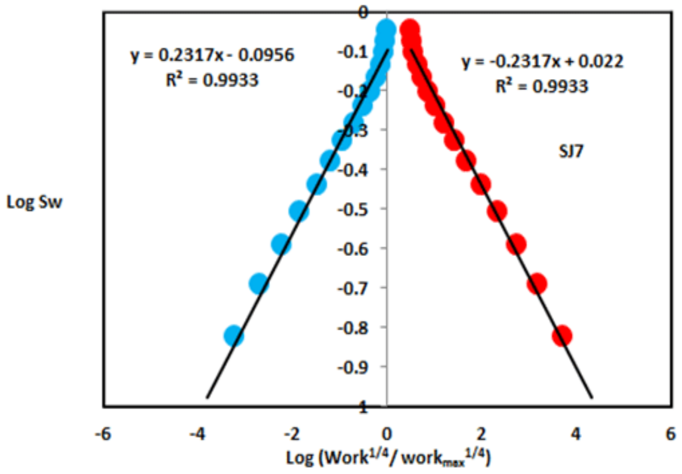

Figure 6. Log (Work$^{1/4}$/Work$^{1/4}_{max}$) & log Pc versus log Sw of sample SJ7.

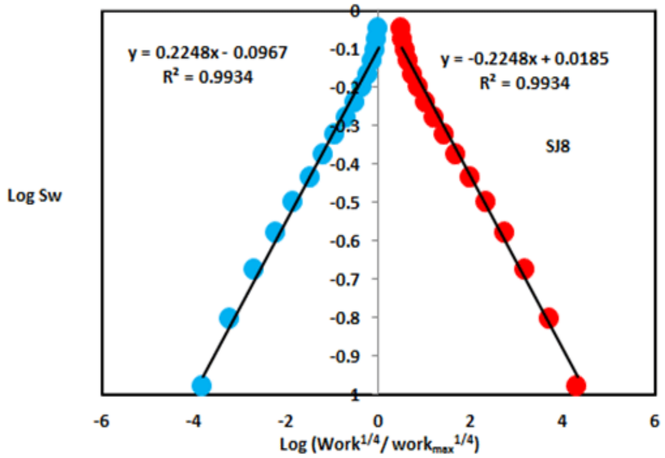

Figure 7. Log (Work$^{1/4}$/Work$^{1/4}_{max}$) & log Pc versus log Sw of sample SJ8.

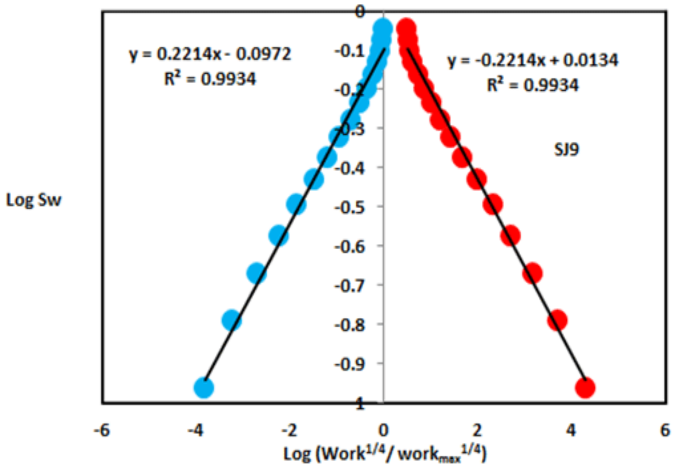

Figure 8. Log (Work$^{1/4}$/Work$^{1/4}_{max}$) & log Pc versus log Sw of sample SJ9.

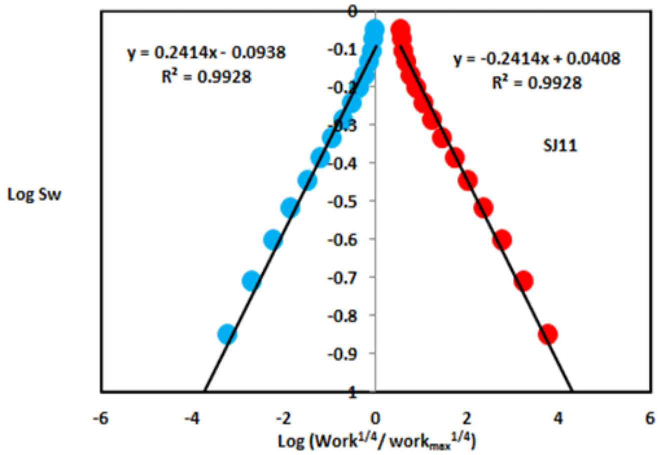

Figure9. Log (Work$^{1/4}$/Work$^{1/4}_{max}$) & log Pc versus log Sw of sample SJ11.

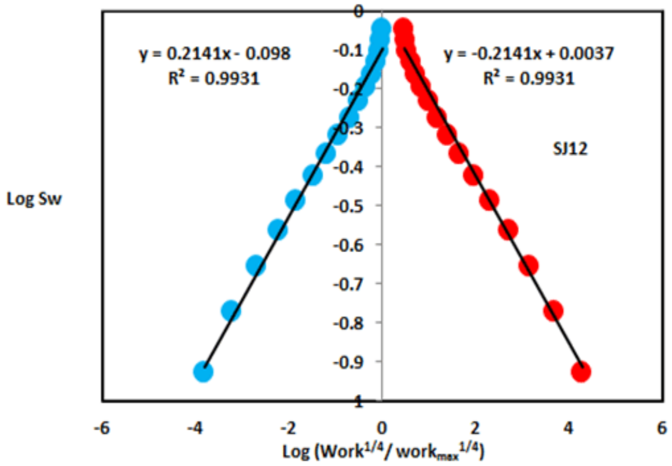

Figure 10. Log (Work$^{1/4}$/Work$^{1/4}_{max}$) & log Pc versus log Sw of sample SJ12.

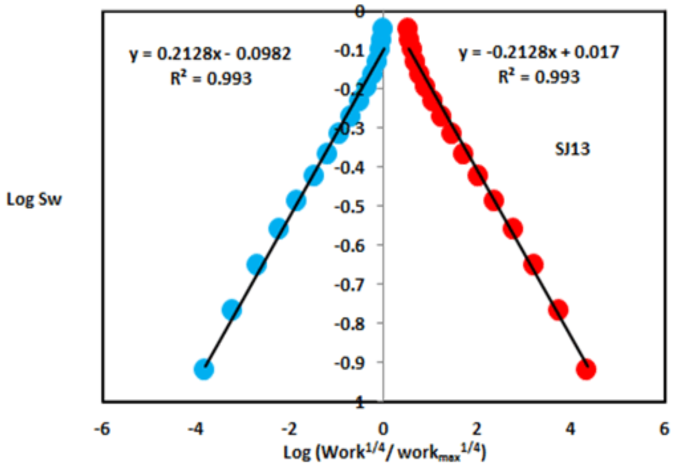

Figure 11. Log (Work$^{1/4}$/Work$^{1/4}_{max}$) & log Pc versus log Sw of sample SJ13.

Overall a plot of positive slope of the first procedure versus negative slope of the second procedure as described in Figure 12 reveals three permeable zones of varying Petro physical properties. These reservoir zone were also confirmed by plotting Work fractal dimension versus capillary pressure fractal dimension as described in Figure 13. Such variation in fractal dimension can account for heterogeneity which is a key parameter in reservoir quality assessment.

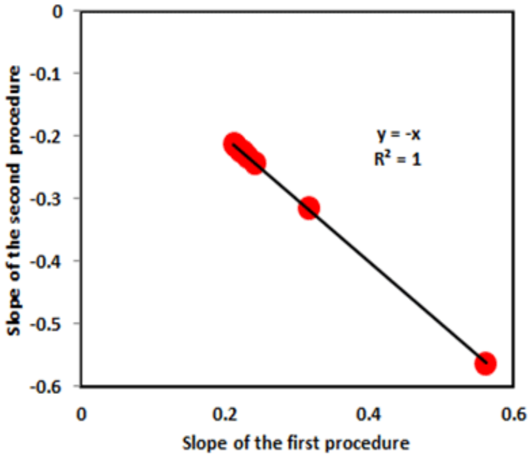

Figure 12. Slope of the first procedure versus slope of the second procedure.

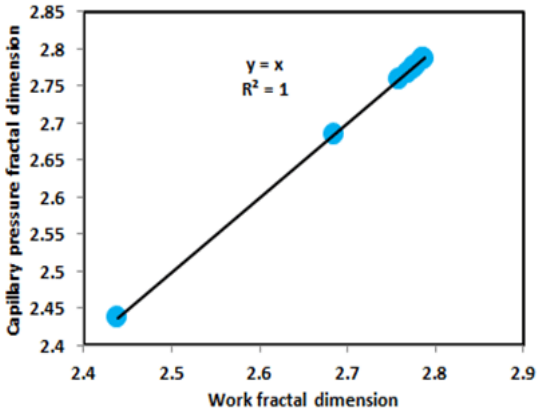

Figure 13. Work fractal dimension versus capillary pressure fractal dimension

Conclusion

The sandstones of the Shajara Reservoirs of the Shajara formation permo-Carboniferous were divided here into three units based on Work fractal dimension. The Units from base to top are: Lower Shajara Work Fractal dimension Unit, Middle Shajara Work Fractal Dimension Unit, and Upper Shajara Work Fractal Dimension Unit. These units were also proved by capillary pressure fractal dimension. The fractal dimension was found to increase with increasing grain size and permeability owing to possibility of having interconnected channels.

Acknowledgement

The author would to thank King Saud University, college of Engineering, Department of Petroleum and Natural Gas Engineering, Department of Chemical Engineering, Research Centre at College of Engineering, and King Abdullah Institute for research and Consulting Studies for their supports.

References

1. Frenkel J (1944) On the theory of seismic and seismoelectric phenomena in a moist soil. J physics 3: 230-241.
2. Li K, Williams W (2007) Determination of capillary pressure function from resistivity data. Transport in Porous Media 67(1): 1-15.
3. Revil A, Jardani A (2010) Seismoelectric response of heavy oil reservoirs: theory and numerical modelling. Geophysical Journal International 180(2): 781-797.
4. Dukhin A, Goetz P, Thommes M (2010) Seismoelectric effect: a non-isochoric streaming current. 1 experiment, J Colloid Interface Sci 345(2): 547-553.
5. Guan W, Hu H, Wang Z (2012) Permeability inversion from low-frequency seismoelectric logs in fluid- saturated porous formations. Geophysical Prospecting 61(1): 120-133.
6. Hu H, Guan W, Zhao W (2012) Theoretical studies of permeability inversion from seismoelectric logs. Geophysical Research Abstracts, 14: EGU2012-6725-1 2012 EGU General Assembly.
7. Borde C, Senechal P, Barriere J, Brito D, Normandin E, et al. (2015) Impact of water saturation on seismoelectric transfer functions: a laboratory study of co-seismic phenomenon. Geophys J Int 200(3): 1317-1335.
8. Jardani A, Revil A (2015) Seismoelectric couplings in a poroelastic material containing two immiscible fluid phases. Geophysical J International 202(2): 850-870.
9. Holzhauer J, Brito D, Bordes C, Brun Y, Guatarbes B (2016) Experimental quantification of the seismoelectric transfer function and its dependence on conductivity and saturation in loose sand. Geophys Prospect 65(4): 1097-1120.
10. Ping R,Wei J-X, Di B-R, Ding P-o, Liu Z-C (2016) Experimental research on seismoelectric effects in sandstone. Applied Geophysics 13(3): 425-436.
11. Djuraev U, Jufar SR, Vasant P (2017) Numerical Study of frequency-dependent seismoelectric coupling in partially-saturated porous media. MATEC Web of Conferences 87: 02001.

12. Alkhidir KEME (2017) Pressure head fractal dimension for characterizing Shajara Reservoirs of the Shajara Formation of the Permo-Carboniferous Unayzah Group, Saudi Arabia. Arch Pet Environ Biotech 2017(2): 1-7.

13. Al-Khidir KE (2018) On Similarity of Pressure Head and Bubble Pressure Fractal Dimensions for Characterizing Permo-Carboniferous Shajara Formation, Saudi Arabia. Journal of Industrial Pollution and Toxicity 1(1): 1-10.

14. Alkhidir KEME (2018) Geometric relaxation time of induced polarization fractal dimension for characterizing Shajara Reservoirs of the Shajara Formation of the Permo-Carboniferous Unayzah Group, Saudi Arabia. Scifed J Petroleum 2(1): 1-6.

15. Alkhidir KEME (2018) Geometric relaxation time of induced polarization fractal dimension for characterizing Shajara Reservoirs of the Shajara formation of the Permo-Carboniferous Unayzah Group-Permo. Int J Pet and Res 2(1): 105-108

16. Alkhidir KEME (2018) Arithmetic relaxation time of induced polarization fractal dimension for characterizing Shajara Reservoirs of the Shajara Formation. Nanosci and Nanotechnol 2(1): 1-8.

17. AlKhidir KEME (2018) Seismo Electric field fractal dimension for characterizing Shajara Reservoirs of the Permo-Carboniferous Shajara Formation Saudi Arabia. Pet petro Chem Eng J 2(4): 1-7.

18. Alkhidir KEME (2018) Resistivity fractal dimension for characterizing Shajara reservoirs of the permo-carboniferous Shajara formation Saudi Arabia. Int J Petrochem Sci and Eng 3(3): 109-112.

19. Alkhidir KEME (2018) Electro Kinetic Fractal Dimension for Characterizing Shajara Reservoirs of the Shajara Formation. Int J Nano Med & Eng 3(4): 1-7.

20. Alkhidir KEME (2018) Electric Potential Energy Fractal Dimension for Characterizing Permo-carboniferous Shajara Formation. Expert Opin Environ Biol 7(2): 1-5.

21. Alkhidir KEME (2018) Electric potential gradient Fractal Dimension for Characterizing Shajara Reservoirs of the Permo-Carboniferous Shajara Formation, Saudi Arabia. Arch Petro Chem Eng (1): 1-6 .

22. Alkhidir KEME (2018) On Similarity of Differential Capacity and Capillary Pressure Fractal Dimensions for Characterizing Shajara Reservoirs of the Permo-Carboniferous Shajara Formation, Saudi Arabia. Scifed Journal of Biofuel and Bioenergetics 1: 1-10.